Attitude Control of a CubeSat in a Circular Orbit using Reaction Wheels

Ajayi Michael Oluwatosin[1,2], Yskandar Hamam[1,2,3] and Karim Djouani[1,4]
ajayimo@tut.ac.za, djouanik@tut.ac.za, hamama@tut.ac.za

[1] F'SATI, Department of Electrical Engineering, Tshwane University of Technology, Staatsartillerie Road, Pretoria West, Pretoria, South-Africa
[2]ESIEE, Paris Est University, France
[3]LISV Laboratory, UVSQ, France
[4]LISSI Laboratory, Paris Est University, France

***Abstract*—This paper presents the attitude control of a CubeSat in a low earth Circular Orbit using Reaction Wheels. Although reaction wheels have certain shortcomings, they provide a fast and accurate approach to achieving attitude stabilization. The objective of this paper is to investigate the performance of reaction wheels for a CubeSat Attitude Control System (ACS). This investigation is achieved via a proposed control law (set point regulator) based on the well known (model independent) PD controller. To validate this objective, two cases for the attitude manoeuvre were considered using SCILAB application software. The numerical computation of the ACS thus helps to provide proper theoretical analysis of the observed results which are provided in this paper to demonstrate the efficiency of the control method.**

Keywords—attitude control system; CubeSat; reaction wheels; PD control

I. INTRODUCTION

CubeSat is a special class of Pico-satellite developed for the purpose of space research and usually has a volume of exactly one litre and weighs no more than one kilogram. California Polytechnic State University (Cal Poly) and Stanford University established the CubeSat Specifications in 1999 to assist universities worldwide to carry out space science and exploration. However, the size of the CubeSat limits the number of actuation system available for its attitude control.
The principal goal of the attitude control system is to stabilize the orientation of the satellite after launch and during the orbital motion of the satellite. They can be divided into two types namely; the passive attitude control system and the active attitude control system. The former can be achieved by using, gravity gradient stabilization, spin stabilization and dual-spin stabilization while the latter utilizes the magnetic torquer, thrusters and reaction wheels. Utilizing reaction wheels for active attitude control of a spacecraft provides a fast, flexible, and accurate way of attitude control and stabilization but certainly not without a disadvantage of being too weighty and expensive. Nevertheless, in [2] a reaction wheel design for CubeSat which takes into account the limitation of the size and weight was proposed.

Reaction wheels are mainly suitable for variable spin rate control and are implemented as special electric motors mounted about the 3-axis of the spacecraft. On the other hand, a tetrahedral configuration of the reaction wheel which includes a fourth axis and hence provides redundancy and also makes it possible to vary its speeds without causing any net torque.

A. Previous Work

Attitude control utilizing reaction wheels have been implemented on very few CubeSat projects. A comprehensive analysis of the attitude control of the BeeSat whose actuation is provided by 3 reaction wheel and 6 magnetic coils was presented in [3] while [4] discusses the design of an attitude control using reaction wheels implemented in SwissCube. In [5] the requirement for a wheel based attitude determination and control system for picosatellites was analyzed. Reference [6], [7] and [8] presented the use of quaternion feedback for attitude control, while [1] proposed a quaternion feedback control system which is globally asymptotically stable (GAS).

In this paper the authors present a model independent PD controller similar to that presented in reference [1] and adapted to work for reaction wheels in a circular orbit. The efficiency and accuracy associated with reaction wheels are

978-1-4673-5943-6/13/$31.00 ©2013 IEEE

verified and simulation results show a good performance of this control method. Hence, the stability of the CubeSat is guaranteed based on the control law adopted using a tetrahedral configuration of the reaction wheel. The circular orbit for this work was achieved via a numerical orbit propagator.

The rest of the paper is organized as follows. The mathematical model of the CubeSat is presented in section II. In section III the controller design is provided. Section IV presents the some simulation results and finally the conclusions/concluding remarks are given in section V.

II. MATHEMATICAL MODELING

The notations and its corresponding descriptions used throughout this paper are given in Table I below.

TABLE I. NOTATIONS AND DESCRIPTIONS

Notation	Description
$\dot{\mathbf{x}}$	Denotes the derivative of a vector $\mathbf{x}$
$\mathbf{S(a)b}$	Matrix representation of cross product operator $\mathbf{a}\times\mathbf{b}$
$\boldsymbol{\omega}_{a,b}^{c}$	Represents the angular velocity of frame b, relative to frame a expressed in frame c
$\mathbf{R}_{a}^{b}$	Denotes the rotation matrix representation of frame a to frame b (i.e. $\mathbf{R}_{o}^{b}$ means rotation from orbit to body)
$\|(.)\|$	Denotes the Euclidean norm and also the induced L_{2-norm} of matrices (spectral norm)
$F_{(.)}$	Symbolizes the coordinate reference frame
$S(3)$	represents the special orthogonal group of order three

a. Table for Notations and Descriptions.

A. Coordinate Reference System

In this paper, three different coordinate frames will be used to represent the orientation of the satellite.

Earth-Centred Inertial Frame – ECI—This reference frame has its origin in the centre of the earth, the x_i- axis is pointing in vernal equinox direction γ. This is in the direction of the vector from the sun through the centre of the earth during vernal equinox. The y_i- axis points 90° east, spanning the equatorial plane and the z_i- axis points through the North Pole. The ECI frame is non – rotating and is assumed fixed in space, i.e. it is an inertial frame in which the Newton's laws of motion apply. This is therefore the frame in which the equation of motion is evaluated. This frame will be denoted F_i.

Spacecraft Orbit Reference Frame—The orbit frame, denoted F_o, will have its origin in the satellites centre of gravity (centre of mass). It is also called the LVLH (Local Vertical Local Horizontal) frame, and could be viewed relatively as a line drawn from the satellite to the centre of earth. In its classification, the z_o- axis will point in vertical line direction towards the earth centre. The x_o- axis points in the direction of the orbital motion parallel to the local horizontal and the y_o- axis is perpendicular to the orbital plane.

Spacecraft body reference frame—This reference frame originate at the satellite centre of gravity (centre of mass), and its basis vectors are aligned with principle axis of inertia. The body frame of the satellite is denoted F_b.

B. Attitude Parameterization

Euler parameters are preferred for attitude parameterization, because of its computational efficiency and non-singularities property. Euler parameters use four variables to represents attitude and it is given as

$$\mathbf{q}=\begin{bmatrix}\eta & \boldsymbol{\varepsilon}^T\end{bmatrix}^T \tag{1}$$

where $\eta=\cos\frac{\theta}{2}$ and $\boldsymbol{\varepsilon}=\begin{bmatrix}\varepsilon_x & \varepsilon_y & \varepsilon_z\end{bmatrix}^T=\mathbf{k}\sin\frac{\theta}{2}$, with $\theta=$ rotation angle about the Eigen-axis, and $\mathbf{k}=\begin{bmatrix}k_1 & k_2 & k_3\end{bmatrix}^T$, is a unitary vector. The unit quaternion must satisfy the constraint $\eta^2+\boldsymbol{\varepsilon}^T\boldsymbol{\varepsilon}=1$.

The rotation matrix from frame b to frame a given in Euler parameter may be written as in [9]

$$\mathbf{R}_{b}^{a}=\mathbf{I}+2\eta\mathbf{S}(\boldsymbol{\varepsilon})+2\mathbf{S}^2(\boldsymbol{\varepsilon}) \tag{2}$$

where $\mathbf{S}(.)$ is the skew symmetric (cross product operator) and can be represented as

$$\mathbf{S}(\boldsymbol{\varepsilon})=\begin{bmatrix}0 & -\varepsilon_z & \varepsilon_y\\ \varepsilon_z & 0 & -\varepsilon_x\\ -\varepsilon_y & \varepsilon_x & 0\end{bmatrix} \tag{3}$$

Generally, the matrix $\mathbf{R}_{o}^{b}$ (i.e. rotation from orbit to body) can be written as:

$$\mathbf{R}_{o}^{b}=\begin{pmatrix}\mathbf{c}_1^b & \mathbf{c}_2^b & \mathbf{c}_3^b\end{pmatrix} \tag{4}$$

where $\mathbf{c}_1^b=\begin{pmatrix}c_{ix}^b & c_{iy}^b & c_{iz}^b\end{pmatrix}^T$ represents the column vector.

C. Kinematics

According to [9] the time derivative of the quaternion elements can be expressed as

$$\dot{\mathbf{q}} = \begin{bmatrix} -\boldsymbol{\varepsilon}^T \\ \eta \mathbf{I}_{3\times 3} + \mathbf{S}(\boldsymbol{\varepsilon}) \end{bmatrix} \boldsymbol{\omega}_{i,b}^b \tag{5}$$

where $\mathbf{I}$ is an identity matrix and $\boldsymbol{\omega}_{i,b}^b$ is the angular velocity of the body frame relative to the inertia frame, expressed in the body frame.

D. Dynamics

Newton's second law for angular motion states that the net external torque $(\boldsymbol{\tau})$ acting on a rigid body (system) equals the time derivative of the angular momentum $(\mathbf{H})$ of the rigid body (system). This is mathematically stated as

$$\boldsymbol{\tau} = \dot{\mathbf{H}}^i \tag{6}$$

Hence, by using the Newton-Euler equations of motion, the dynamic model of a rigid body may be expressed as

$$\dot{\boldsymbol{\omega}}_{i,b}^b = \mathbf{J}^{-1}\left[-\mathbf{S}\left(\boldsymbol{\omega}_{i,b}^b\right)\mathbf{J}\boldsymbol{\omega}_{i,b}^b + \boldsymbol{\tau}\right] \tag{7}$$

where $\boldsymbol{\omega}_{i,b}^b \in \Re^3$ is the angular velocity of the body frame relative to the inertial (ECI) frame expressed in the body, while $\mathbf{J} \in \Re^{3\times 3}$ is the inertia matrix, $\boldsymbol{\tau} \in \Re^3$ is the net external torque acting on the body and may be expressed as

$$\boldsymbol{\tau} = \boldsymbol{\tau}_c + \boldsymbol{\tau}_d \tag{8}$$

where $\boldsymbol{\tau}_c$ is the control torque and $\boldsymbol{\tau}_d$ is the disturbance torque.

A complete description of the dynamical model may therefore be derived from (7), and (8) giving

$$\dot{\boldsymbol{\omega}}_{i,b}^b = \mathbf{J}^{-1}\left[-\mathbf{S}(\boldsymbol{\omega}_{i,b}^b)\mathbf{J}\boldsymbol{\omega}_{i,b}^b + \boldsymbol{\tau}_c + \boldsymbol{\tau}_d\right] \tag{9}$$

The angular velocity of the model in the body frame relative to the orbit frame may be derived as

$$\boldsymbol{\omega}_{o,b}^b = \boldsymbol{\omega}_{i,b}^b - \mathbf{R}_i^b \boldsymbol{\omega}_{i,o}^i \tag{10}$$

where $\mathbf{R}_i^b$ is the rotation matrix from the inertial (ECI) frame to the body frame while $\boldsymbol{\omega}_{i,o}^i$ is the angular velocity of the orbit frame relative to the inertial (ECI) frame and mathematical expressed as

$$\boldsymbol{\omega}_{i,o}^i = [0 \quad -\omega_o \quad 0]^T \tag{11}$$

where $\omega_o = \sqrt{\mu / R^3}$ and R is the mean radius .

It should be noted that applying the rotation matrix $\mathbf{R}_i^b = \left(\mathbf{R}_b^i\right)^{-1}$ gives the rotation from the inertial (ECI) frame to body frame.

E. Reaction Wheels

Reaction wheels are basically rotors rotated by an electric motor. The motor applies a torque to reduce or increase the speed of the rotor which results into a reacting torque in the body of the spacecraft. This is reacting torque causes the spacecraft to spin in the opposite way of the reaction wheel rotation in a proportional amount by conservation of angular momentum. 3-axis stabilization can be achieved by utilizing 3 reaction wheels. However, the tetrahedral configuration provides a four reaction wheel system which makes it possible for the reaction wheels speed to be changed without causing any net torque. This also provides redundancy. The mathematical expression of the actuating torquer for tetrahedral configuration can be expressed as in [10]

$$\mathbf{T} = \begin{bmatrix} 0 & 0 & \frac{1}{3}\sqrt{6} & -\frac{1}{3}\sqrt{6} \\ 0 & -\frac{2}{3}\sqrt{2} & \frac{1}{3}\sqrt{2} & \frac{1}{3}\sqrt{2} \\ -1 & \frac{1}{3} & \frac{1}{3} & \frac{1}{3} \end{bmatrix} \tag{12}$$

F. Aerodynamics Torque

When the upper atmosphere interacts with the spacecraft's surface a torque is produced about the centre of mass. The effectiveness of this torque depends on the area and shape of the exposed surface. This disturbance torque has little effect on spacecraft operating at high altitude while for low orbit spacecraft the air density is high enough to influence the attitude dynamics of the body. The calculation of the aerodynamic torques may be done by representing the spacecraft as a collection of simple geometrical elements. The torque about the centre of mass of the spacecraft is the vector sum of the individual torques for each of these geometrical simplifications and it is written as in [11]

$$\boldsymbol{\tau}_{aero} = \sum\nolimits_k \mathbf{S}(\mathbf{r}_k)\mathbf{F}_{aero,k} \tag{13}$$

where $\mathbf{r}_k$ is the vector distance from the centre of mass to the centre of pressure to the specific geometric shape and $\mathbf{F}_{aero,k}$ is the force acting on the component.

G. Gravity Gradient Torque

Gravity gradient torque experienced on the spacecraft is the resultant effect of the variation in force of gravity exerted on different parts of a spacecraft body. The effect of this disturbance torque is greater in magnitude at the Low earth

orbit (LEO), which causes the spacecraft to experience a pull towards Earth and may be expressed as in [12]

$$\boldsymbol{\tau}_g = \frac{3\mu}{R^3}\mathbf{S}\left(\mathbf{c}_3^b\right)\mathbf{J}\mathbf{c}_3^b \tag{14}$$

where $\mathbf{J}$ is the inertia matrix of the spacecraft, $\mu = 398600 km^3/s^2$ is the gravitational constant of the Earth and $\mathbf{c}_3^b$ is the vector projection of the z_o axis in the body frame.

III. CONTROLLER DESIGN

The model independent PD control law similar to that of [1] was incorporated with an intention to controlling the attitude of the spacecraft.

A. Problem Statement

The problem addressed in this work is the design of a controller that is capable of driving the spacecraft to stability i.e. the initial attitude $\mathbf{q}$ to the desired $\mathbf{q}_d$ thus satisfying the kinematic equation

$$\dot{\mathbf{q}}_d = \begin{bmatrix} -\boldsymbol{\varepsilon}_d^T \\ \eta_d \mathbf{I}_{3\times 3} + \mathbf{S}(\boldsymbol{\varepsilon}_d) \end{bmatrix} \boldsymbol{\omega}_{i,b}^d \tag{15}$$

where $\boldsymbol{\omega}_{i,b}^d$ is the desired angular velocity of the body frame relative to the inertial frame.

B. Quaternion Error

The quaternion error $\mathbf{q}_e$ may be expressed as in [9]

$$\mathbf{q}_e = \overline{\mathbf{q}}_d \otimes \mathbf{q} = \begin{bmatrix} \eta_d & \boldsymbol{\varepsilon}_d^T \\ -\boldsymbol{\varepsilon}_d & \eta_d \mathbf{I}_{3\times 3} - \mathbf{S}(\boldsymbol{\varepsilon}_d) \end{bmatrix} \mathbf{q} \tag{16}$$

where $\overline{\mathbf{q}}_d$ is the desired quaternion complex conjugate and $\mathbf{q}$ is the initial attitude.

The equivalent quaternion representation of attitude $\mathbf{q}_e$, with $\mathbf{q}_e = \begin{bmatrix} \pm 1 & \mathbf{0}^T \end{bmatrix}^T$ corresponding to the equilibrium point differs mathematically by a rotation of 360° between the negative and positive axis, hence the equilibrium is chosen to be $\mathbf{q}_e = \begin{bmatrix} 1 & \mathbf{0}^T \end{bmatrix}^T$. However, It is shown in [1] that in the event where $\eta = -1$ corresponds to an unstable equilibrium and any small perturbation will cause a rotation of 360° to $\eta = +1$.

C. Control Law

We achieved this control effect by using the control law

$$\boldsymbol{\tau}_c = -\left(\mathbf{K}_p \boldsymbol{\varepsilon}_e + \mathbf{K}_d \Delta\boldsymbol{\omega}_{i,b}^b\right) \tag{17}$$

where $\boldsymbol{\varepsilon}_e = \begin{bmatrix} \varepsilon_{ex} & \varepsilon_{ey} & \varepsilon_{ez} \end{bmatrix}^T$ corresponds to the vector in the quaternion error $\mathbf{q}_e$, $\Delta\boldsymbol{\omega}_{i,b}^b = \boldsymbol{\omega}_{i,b}^b - \boldsymbol{\omega}_{i,b}^d$ is the angular velocity error, $\mathbf{K}_p$ and $\mathbf{K}_d$ are positive gain matrices. $\mathbf{K}_p = k\,\mathrm{sgn}(\eta_e)\mathbf{I}$, $\mathbf{K}_d = \mathrm{diag}(K_{d1}, K_{d2}, K_{d3})\ k$, K_{d1}, K_{d2}, K_{d3} are constants and $\mathbf{I}$ an identity matrix. The signum function $\mathrm{sgn}(\eta_e)$ is a function that returns 1 for values of (η_e) equal to or greater than 0 and -1 for negative values of (η_e) mathematically written as

$$\mathrm{sgn}(\eta_e) = \begin{cases} -1, & \text{if } \eta_e < 0 \\ 1, & \text{if } \eta_e \geq 0 \end{cases} \tag{18}$$

A closed loop system is achieved when (17) is introduced into (9), which is given below as

$$\dot{\boldsymbol{\omega}}_{i,b}^b - \mathbf{J}^{-1} - \mathbf{S}\left(\boldsymbol{\omega}_{i,b}^b\right)\mathbf{J}\boldsymbol{\omega}_{i,b}^b + \left(\mathbf{K}_p\boldsymbol{\varepsilon}_e + \mathbf{K}_d\Delta\boldsymbol{\omega}_{i,b}^b\right) + \boldsymbol{\tau}_d = 0 \tag{19}$$

The stability proof given in [1] is done by considering the model independent PD control law and letting

$$\rho_1 \equiv \left\|\dot{\boldsymbol{\omega}}_{i,b}^d\right\| + \left\|\boldsymbol{\omega}_{i,b}^d\right\|^2 \tag{20}$$

if $\rho_1 \in L_2[0 \quad \infty) \cap L_\infty[0 \quad \infty)$ then $\boldsymbol{\varepsilon}_e$ and $\Delta\boldsymbol{\omega}_{i/o,b}^b \to 0$ as $t \to \infty$. Since this implementation could be carried out either by using the body frame or the inertial frame [1].

By employing the Lyaponuv candidate function defined as

$$V = \left(\mathbf{K}_p + c\mathbf{K}_d\right)\left((\eta - 1)^2 + \boldsymbol{\varepsilon}_e \cdot \boldsymbol{\varepsilon}_e\right) + \frac{1}{2}\Delta\boldsymbol{\omega}_{i,b}^b \cdot \mathbf{J}\Delta\boldsymbol{\omega}_{i,b}^b -$$

$$c\boldsymbol{\varepsilon}_e \cdot \mathbf{J}\Delta\boldsymbol{\omega}_{i,b}^b \tag{21}$$

$$V \geq \mathbf{x}^T \mathbf{P}_c \mathbf{x} \tag{22}$$

where

$$\mathbf{x} = \begin{bmatrix} \|\boldsymbol{\varepsilon}_e\| \\ \left\|\Delta\boldsymbol{\omega}_{i,b}^b\right\| \end{bmatrix} \quad \mathbf{P}_c = \frac{1}{2}\begin{bmatrix} 2(\mathbf{K}_p + c\mathbf{K}_d) & c\|\mathbf{J}\| \\ c\|\mathbf{J}\| & \mu_{\mathbf{J}} \end{bmatrix}$$

and

$$\mu_{\mathbf{J}} \leq \|\mathbf{J}\|$$

Computing the time derivative of (21) and substituting the model independent PD control law into it gives

$$\dot{V} = -c\mathbf{K}_p\left\|\boldsymbol{\varepsilon}_e\right\|^2 - \mathbf{K}_d\left\|\Delta\boldsymbol{\omega}_{i,b}^b\right\|^2 + \left(\Delta\boldsymbol{\omega}_{i,b}^b - c\boldsymbol{\varepsilon}_e\right)\cdot\left(-\mathbf{S}\left(\boldsymbol{\omega}_{i,b}^d\right)\mathbf{J}\boldsymbol{\omega}_{i,b}^d - \mathbf{J}\dot{\boldsymbol{\omega}}_{i,b}^d\right)$$
$$-c\Delta\boldsymbol{\omega}_{i,b}^b\cdot\mathbf{J}\left(\mathbf{S}\left(\frac{1}{2}\Delta\boldsymbol{\omega}_{i,b}^b\right)\boldsymbol{\varepsilon}_e - \frac{1}{2}\eta\Delta\boldsymbol{\omega}_{i,b}^b + \mathbf{S}\left(\boldsymbol{\omega}_{i,b}^d\right)\right)\boldsymbol{\varepsilon}_e -$$

$$c\boldsymbol{\varepsilon}_e\cdot\left(\mathbf{S}\left(-\boldsymbol{\omega}_{i,b}^b\right)\mathbf{J}\Delta\boldsymbol{\omega}_{i,b}^d - \left(\mathbf{S}\left(\boldsymbol{\omega}_{i,b}^d\right)\Delta\boldsymbol{\omega}_{i,b}^b\right)\mathbf{J}\right)$$
$$\le -\mathbf{x}^T\mathbf{Q}_c\mathbf{x} + \mathbf{w}^T\mathbf{x}$$
$$\le -\lambda\left\|\mathbf{x}\right\|^2 + \rho\left\|\mathbf{x}\right\| \qquad (23)$$

where

$$\mathbf{Q}_c \equiv \begin{bmatrix} c\mathbf{K}_p & \frac{3}{2}\left\|\mathbf{J}\right\|\gamma_d c \\ \frac{3}{2}\left\|\mathbf{J}\right\|\gamma_d c & \mathbf{K}_d - c\left\|\mathbf{J}\right\| \end{bmatrix} \qquad (24)$$

$$\mathbf{w} \equiv \left\|\mathbf{J}\right\|\left(\left\|\dot{\boldsymbol{\omega}}_{i,b}^d\right\| + \left\|\boldsymbol{\omega}_{i,b}^d\right\|^2\right)\begin{bmatrix}1\\ c\end{bmatrix} \qquad (25)$$

$$\rho \equiv \sqrt{1+c^2}\left\|\mathbf{J}\right\|\left(\left\|\dot{\boldsymbol{\omega}}_{i,b}^d\right\| + \left\|\boldsymbol{\omega}_{i,b}^d\right\|^2\right) \qquad (26)$$

$\gamma_d \equiv \sup\left\|\boldsymbol{\omega}_{i,b}^d\right\|$ and $\lambda \equiv \lambda_{\min}\left(\mathbf{Q}_c\right)$ is the minimum Eigenvalue of $\mathbf{Q}_c$. $\mathbf{Q}_c$ has been modified according to [13].

Based on several mathematical manipulations and the application of certain stability and Lyapunov arguments according to [1], it was shown that the zero equilibrium of the control law is globally asymptotically stable (GAS) bearing in mind that the equilibrium points have been forced to only one point (problem associated with representing attitude with quaternion). This is done by showing that $\mathbf{x} \in L_2[0 \quad \infty)$ and that c is kept small enough to make $\mathbf{P}_c$ and $\mathbf{Q}_c$ positive definite. It should be stated at this point that the control law presented does not guarantee a continuous (GAS) vector field on $S(3)X\Re^3$. However, on $S(3)X\Re^3$ where $S(3)$ is the unit sphere in $\Re^4$ where the quaternion lies, a (GAS) vector field in the closed-loop can be found. The controller may have its short-comings but very useful in the event where $\omega_{i/o,b}^d = 0$ [14].

D. Reaction Wheel Torque

The system of four reaction wheel is designed to provide 3-axis control stabilization and have the tendency of compensating for a failed reaction wheel axis. The reaction wheel torque is designed by the mathematical expression

$$\boldsymbol{\tau}_w = \mathbf{T}^T\boldsymbol{\tau}_c \qquad (27)$$

where $\boldsymbol{\tau}_c$ is the control torque derived from the control law in equation (17). $\mathbf{T} \in \Re^{4\times3}$ is the tetrahedral configuration allocation matrix.
The required torque (regulator) can be expressed as

$$\boldsymbol{\tau}_r = \boldsymbol{\tau}_{\max}\mathbf{R}_{ob}^b noise \qquad (28)$$

where $\boldsymbol{\tau}_{\max}$ is the maximum actuator torque and $\mathbf{R}_{ob}^b$ is the rotation matrix of the body frame to the orbit frame in the body frame.

IV. SIMULATIONS

The simulation parameters used in this paper are given in Table II. SCILAB was used to carry out this numerical simulation and the gains of the PD controller were selected (tuned) manually. The maximum actuator torque was calculated based on the analysis in [2] so as to overcome the limitation of the size and weight of the reaction wheels. A percentage of a uniformly distributed noise designed to give a realistic disturbance effect on the torque was added to this torque as in [11]. Two (2) cases were presented to evaluate the attitude tracking control ability of the control method.

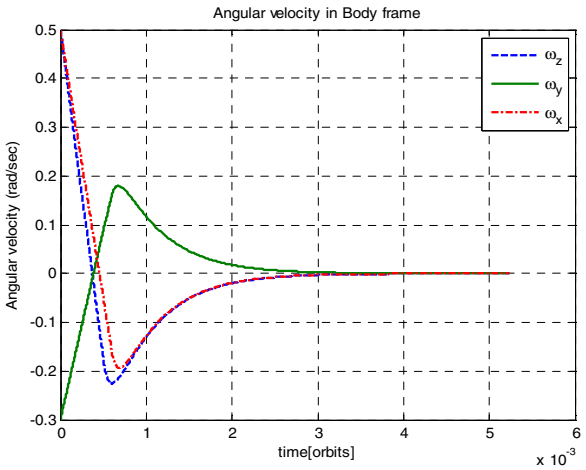

Figure 1. Simulation of the Angular velocity in Body frame

TABLE II. SIMULATION PARAMETERS

Parameter	Value
Inertia matrix, $\mathbf{J}$	$1.87\times10^{-3}\mathbf{I}kgm^3$
Angular velocity $\boldsymbol{\omega}_{o,b}^{b}$	$[0.3 \quad -0.5 \quad 0.3]^T rad/\sec$
k	2.5×10^{-3}
$\mathbf{K}_d$	$4.8\times10^{-3}\mathbf{I}$
$\boldsymbol{\tau}_{aero}$	$3.42\times10^{-9}\,Nm$
$\boldsymbol{\tau}_{\max}$	$0.000268\,Nm$
Inclination, i	60°
Eccentricity, e	1.68×10^{-4}
Semimajor axis, a	$6919.2km$
Right ascension of ascending node, Ω	0°
Argument of perigee, ϖ	0°
True anomaly, ν	0°
Orbital period, p	5732s (1 orbit)

b. Table for Simulation Parameters

Case 1: Initial attitude $[Z\ Y\ X]=[10 \quad -20 \quad 30]^T$ deg and the Desired attitude $[Z\ Y\ X]=[0 \quad 0 \quad 0]^T$ deg .

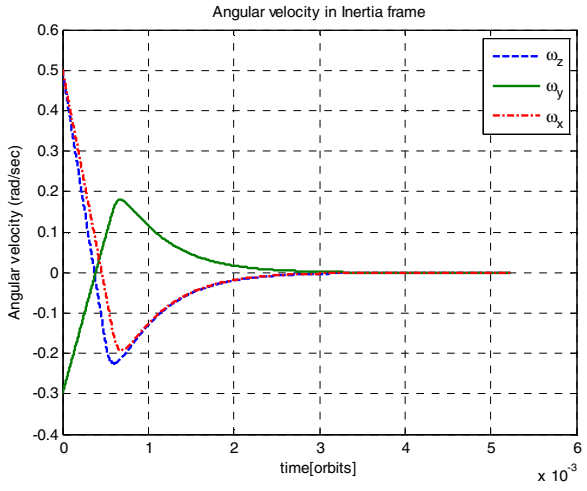

Figure 2. Simulation of the Angular velocity in Inertia frame

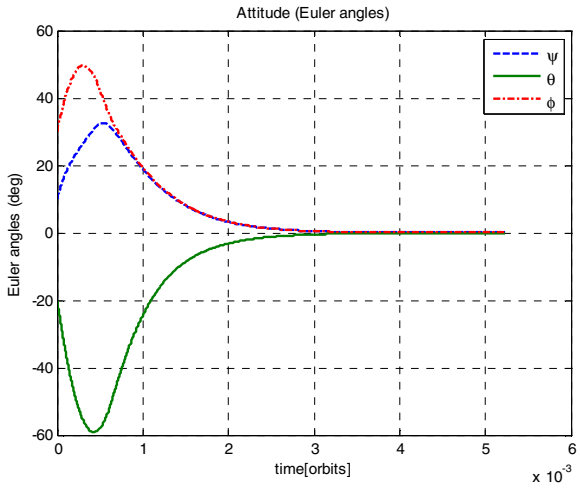

Figure 3. Simulation of the Attitude in Euler angles

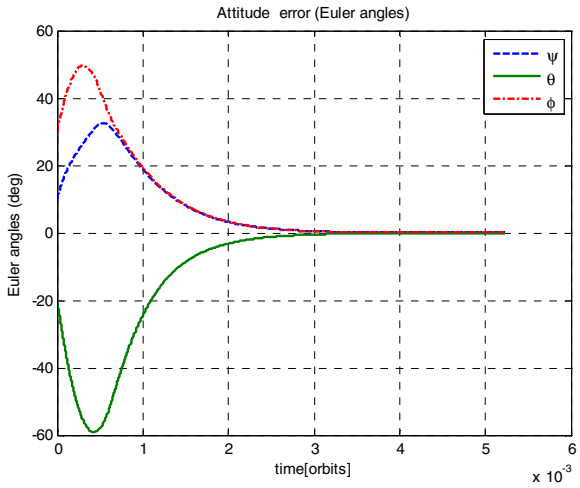

Figure 4. Simulation of the Attitude error in Euler angles

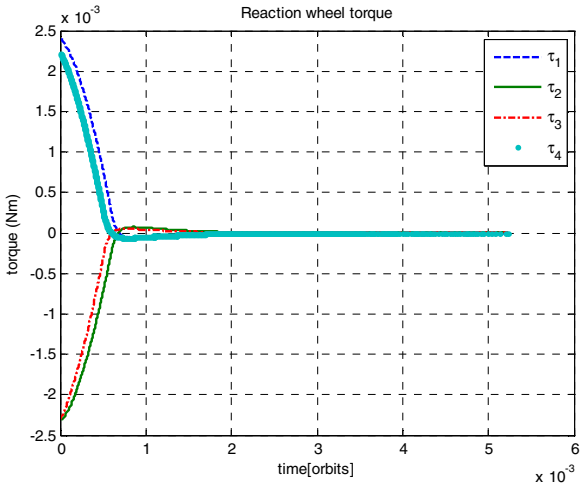

Figure 5. Simulation of the Reaction Wheel torque

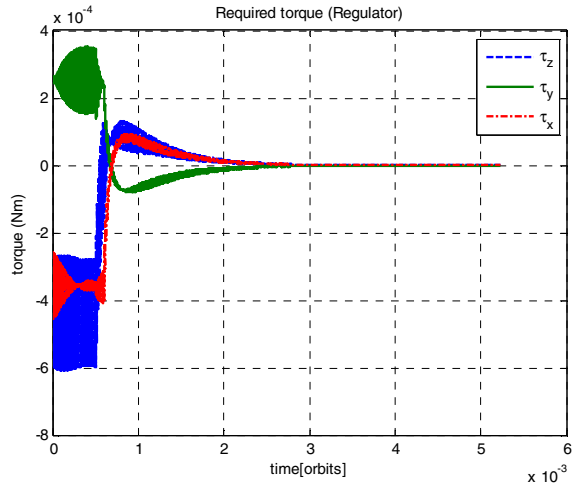

Figure 6. Simulation of the Regulator

Case 2: Initial attitude $[Z\ Y\ X] = [0 \quad 0 \quad 0]^T$ deg and the Desired attitude $[Z\ Y\ X] = [10 \quad -20 \quad 30]^T$ deg .

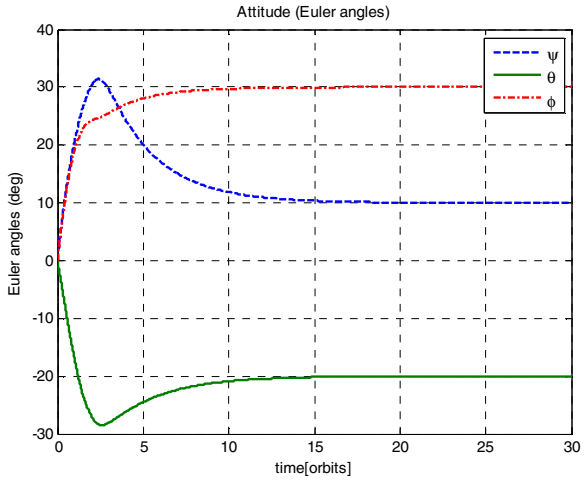

Figure 7. Simulation of the Attitude in Euler angles

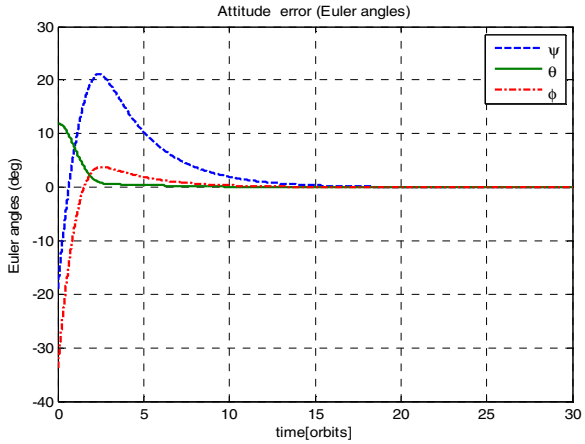

Figure 8. Simulation of the Attitude error in Euler angles

A. Results

Case 1:

Figures 1 and 2 represents the angular velocity in the body frame and inertia frame respectively; the plot shows the trajectories of the angular velocities of the 3 axis converging to zero at a value near 0.003 orbits. This proves that the control torques have the ability to control the attitude of the spacecraft, else with no control on the spacecraft the angular velocity has a tendency of growing uncontrollably to infinity. In Figures 3 and 4 the simulation results of the attitude and attitude error in Euler angles was presented. This proves that the trajectory can converge to the desired point within a minima (fast) time. This feature is well known with reaction wheels. Figures 5 and 6 stands for the required torque (regulator) and the reaction wheel torque respectively. The trajectory of the required torque (regulator) converges to zero properly at about 0.003 orbits and it can be observed that the maximum torque is not exceeded. This result shows that the torques induced by the controller was able to bring the spacecraft to convergence at about 0.003 orbits.

From these plots the control method via the reaction wheels can be assumed to guarantee the 3-axis control and convergence of the closed-loop system to the desired equilibrium point. At 0.003 orbits the attitude of the spacecraft starts to converge to zero (stability). The disturbance effect cannot be seen on the plots which show the controller-actuator robustness.

Case 2:

The attitude was reversed in this case to validate the attitude tracking control capability and thus figures 7 and 8 emanated. Figure 7 represents the attitude in Euler angles and the trajectories of the 3 axis can be seen to perfectly reach their respective desired values at about 0.015 orbits. The difference of time between case 1 and case 2 is as a result of the difference in desired attitude. While the plot in figure 8 proves that the error of the states reaches zero.

V. CONCLUSIONS

In this paper the authors were able to investigate the fast and accurate attributes of the reaction wheels when used as an actuation means in attitude control system. A model independent PD control law integrated to work for reaction wheels only was used to achieve this purpose. Based on the results obtained, it can be seen that attitude regulation can be achieved using reactions wheels at a very precise and fast rate even in the presence of certain disturbance effects.

REFERENCES

[1] J. T. Y. Wen and K. Kreutz-Delgado, "The attitude control problem," *IEEE Transactions on Automatic Control, ,* vol. 36, pp. 1148-1162, 1991.

[2] E. Oland and R. Schlanbusch, "Reaction wheel design for CubeSats," *4th International Conference on Recent Advances in Space Technologies, RAST '09*, 2009, pp. 778-783.

[3] H. Kayal, F. Baumann, K. Briess, "BEESAT - A Pico Satellite of TU Berlin for the In-Orbit Verification of Miniaturised Wheels," *International Astronautical Conference,* 2008.

[4] G. Bozovic, "SwissCube: development of an ultra-light and efficient Inertia Wheel for the attitude control and stabilization of CubeSat class satellites", *International Astronautical Conference*, 2008.

[5] M. C. G. Angel. *Reaction Wheels for Picosatellites, Master's thesis, Department of Space Science, Continuation Courses Space Science and Technology, Lulea University of Technology, Kiruna, 2009*.

[6] H. Weiss, "Quaternion-based rate/attitude tracking system with application to gimbal attitude control," *Journal of Guidance Control Dynamics,* vol. 16, pp. 609-616, 1993.

[7] B. Wie, H. Weiss, A. Arapostathis, "Quaternion feedback regulator for spacecraft eigenaxis rotations". *Journal of Guidance*, 12 (1989), pp. 375–380, 1989.

[8] B. Wie and P. M. Barba, "Quaternion feedback for spacecraft large angle maneuvers," 1984.

[9] O. Egeland and J. T. Gravdahl. *Modelling and Simulation for Automatic Control, Marine Cybernetics, Trondheim, Norway, 2002*.

[10] C. Kaplan. *Leo Satellites: Attitude Determination and Control components; some linear attitude control techniques, Master's thesis, Department of Electrical Engineering, Middle East Technical University, 2006*.

[11] H. Oyvind. *Attitude Control by means of Explicit Model Predictive Control, via Multi-parametric Quadratic Programming, Master's thesis, Department of Engineering Cybernetics, Norwegian University of Science and Technology, 2004*.

[12] M. J. Sidi, *Spacecraft dynamics and control: a practical engineering approach* vol. 7: Cambridge Univ Pr, 2000.

[13] O. E. Fjellstad and T. I. Fossen, "Comments on “The attitude control problem&rdquo," *IEEE Transactions on Automatic Control,* vol. 39, pp. 699-700, 1994.

[14] K. K. Tonne. *Stability analysis of EKF-based Attitude Determination and Control, Master's thesis, Department of Engineering Cybernetics, Nowegian University of Science and Technology, 2007*.